

Synergistic Photocatalytic Removal of Methyl Orange Using Ni-Substituted BiFeO₃ Nanostructures under UV Irradiation

Razieh Sanavi Khoshnood^{1*}, Sadaf Fathi¹

¹ Department of Chemistry, Mashhad Branch, Islamic Azad University, Mashhad, Iran

* E-mail: rskhoshnood@yahoo.com

Received 12 July 2025; accepted 13 September 2025

Abstract

Methyl orange dye is a stable, non-degradable, and water-soluble compound, and its removal from the environment is possible with conventional water treatment methods. In this study, bismuth ferrite nanoparticles substituted with nickel BiFe_{1-x}Ni_xO₃ (x= 0.00, 0.01, 0.03 & 0.05) were synthesized by the sol-gel method. This research was conducted to investigate the photocatalyst effect of bismuth ferrite nanoparticles in the degradation of methyl orange (MO) dye. The characteristics of the nanoparticles were determined by scanning electron microscopy (SEM), Fourier transform infrared (FT-IR), and X-ray diffraction (XRD) analysis—with Methyl orange dye as a pollutant in this study. The selection and effect of different parameters in the photocatalytic degradation of methyl orange dye, including dye concentration, pH, the number of nanoparticles, and the irradiation time, were investigated and optimized. The findings of the research show the effectiveness of bismuth ferrite nanoparticles in the destruction of metallic orange color with a concentration of 3 mg/liter, solution pH 2, number of nanoparticles 0.1 g, and irradiation time of 120 minutes under a mercury lamp. The percentage of destruction of metallic orange color for nanoparticles (x= 0.00, 0.01, 0.03 & 0.05) BiFe_{1-x}Ni_xO₃ are: 60.48, 74.44, 76.33 and 75.82, respectively.

Keywords : photocatalyst – Bi-Ni Nano ferrites– méthyl orange – sol-gel

1. Introduction

Water, as one of the vital elements, is not only essential for the physical survival of humans but also plays a significant role in domestic and industrial activities. However, uncontrolled pollution of water resources has become a serious challenge in water resource management [1]. Population growth, industrial development, and agricultural activities have caused a substantial decline in clean water resources worldwide, highlighting the critical importance of water treatment and recycling.[2]. Among various industries, the textile industry is considered a major source of water pollution due to its high-water consumption and extensive use of chemical dyes, especially azo dyes. The discharge of wastewater containing chemical dyes such as methyl orange, due to their high stability and significant toxicity, poses serious environmental problems. Effective removal of these pollutants from wastewater prior to their release into natural aquatic environments is essential.[3]. Methyl orange, an organic azo dye, is widely used in wastewater treatment studies. This dye contains an azo group (-N=N-) linked to two aromatic rings, and its presence in water sources can cause

considerable environmental issues. Industrial wastewater discharge containing this dye leads to significant contamination of groundwater resources and threatens aquatic life. Colored pollutants absorb sunlight at the water surface, preventing light penetration into lower layers, which reduces dissolved oxygen levels and results in the death of aquatic organisms [4, 5]. Therefore, removal of dyes from industrial wastewater before entering natural water bodies is crucial for preserving aquatic ecosystems. Photocatalytic processes using nano photocatalysts under visible light irradiation have emerged as an efficient approach for degrading organic pollutants. Bismuth ferrite (BiFeO₃ or BFO), a multiferroic material exhibiting both ferroelectric and antiferromagnetic properties at room temperature, has attracted attention due to its photocatalytic [6] activity under visible light, thermal and chemical stability, and facile magnetic separability. Nevertheless, limitations such as rapid recombination of electron-hole pairs and relatively wide band gap restrict its photocatalytic efficiency to enhance the properties of BFO, various strategies including doping with transition metal ions, composite synthesis, and surface modification have been employed. Nickel (Ni²⁺) doping is particularly effective due to its ionic radius similarity to Fe³⁺ and its ability to

induce structural and electronic modifications. Incorporation of nickel into the BFO lattice reduces the band gap, suppresses carrier recombination, and improves material stability.

Several synthesis methods have been reported for producing size-controlled BFO nanoparticles, including sol-gel, liquid phase sintering, hydrothermal, solid-state reaction, laser ablation, electrospinning, and magnetron sputtering. Among these, the sol-gel method has garnered considerable interest owing to its simplicity, low cost, uniform molecular-level elemental distribution, and structural stability. This method has been further developed into subtypes such as citric acid-assisted sol-gel, ethylene glycol method, tartaric acid-assisted sol-gel, and polyvinyl alcohol-ethylene glycol composite techniques [7]. The use of tartaric acid as a complexing agent in the sol-gel process plays a key role in improving nanoparticle quality by forming stable and uniform complexes with Bi^{3+} and Fe^{3+} ions [8, 9], preventing premature precipitation, and enhancing the purity and homogeneity of the final product. Additionally, this approach allows sintering at lower temperatures and reduces the formation of secondary phases [10]. In this study, nickel-doped BiFeO_3 nanoparticles were synthesized via the tartaric acid-assisted sol-gel method, and their efficiency in removing methyl orange dye from industrial wastewater was investigated. To optimize the dye degradation process, parameters including irradiation type, solution pH, nanoparticle dosage, and irradiation time were examined and adjusted. The results demonstrate that nickel doping combined with tartaric acid-assisted synthesis significantly enhances photocatalytic activity, reduces the band gap, and increases the specific surface area, leading to improved removal efficiency of organic pollutants. These novel materials represent an effective, economical, and environmentally friendly option for wastewater treatment.

2- Experimental

2-1- Materials

In this study, the sol-gel process, due to its advantages in synthesizing nano powders, was employed for the synthesis of rhombohedral perovskite-structured bismuth ferrite and nickel-substituted bismuth ferrite ($\text{BiFe}_{1-x}\text{Ni}_x\text{O}_3$).

2-2- Chemicals and Apparatus

The materials used in this research include: bismuth (III) nitrate pentahydrate (99%), iron (III) nitrate nonahydrate (99%), tartaric acid (99% purity) supplied by MERCK, nickel (II) nitrate hexahydrate (99% purity) supplied by FLUKA, nitric acid (65% purity) from RIEDEL-DEHAEN, and methyl orange purchased from MERCK. The vibrational spectra of the samples, prepared in solid form as KBr pellets, were analyzed using a

spectrophotometer (Avatar.370-FT-IR Thermo Nicolet) in the range of $400\text{--}4000\text{ cm}^{-1}$. Crystal structures and material identification were examined using an XRD device (Philips Analytical X-Ray B.V). The surface morphology of the nanoparticles was studied with a field emission scanning electron microscope (FE-SEM, HITACHI S-4160).

A drying oven (Pars Azma Co.) and an electric furnace (SCI FINETECH) were utilized for drying the samples. Solution mixing and temperature application were performed using a magnetic stirrer (Heidolph MR Hei), and pH measurements were conducted with a pH meter (Metrohm). A Sartorius digital balance was used for weighing, and a photochemical reactor was employed for irradiation to investigate solution changes. The removal of dyes was monitored using a UV-Vis spectrophotometer (Varian, Cary Bio50).

2-3- Synthesis of BiFeO_3

In this study, BFO nanoparticles were synthesized using the sol-gel method with tartaric acid [11]. To prepare this compound, 20 mL of deionized water was added to a beaker, followed by the addition of 1 mL of concentrated nitric acid. Then, 2.02 g of $\text{Fe}(\text{NO}_3)_3 \cdot 9\text{H}_2\text{O}$ was dissolved in the solution, and after obtaining a clear solution, 2.52 g of $\text{Bi}(\text{NO}_3)_3 \cdot 5\text{H}_2\text{O}$ was added, resulting in a completely transparent solution. After 2 hours, 1.5 g of tartaric acid ($\text{C}_4\text{H}_6\text{O}_6$) was added to the solution, leading to the formation of a colloidal mustard-coloured solution [12,13]. Subsequently, ammonia was added to adjust the pH to 3. The materials were then ground and placed in a crucible, which was heated in a furnace at 400°C for 3 hours. After washing with nitric acid, the crucible was heated at 650°C in the furnace and finally subjected to XRD analysis.

2-4- Synthesis of $\text{BiFe}_{1-x}\text{Ni}_x\text{O}_3$

To prepare $\text{BiFe}_{1-x}\text{Ni}_x\text{O}_3$ ($x = 0.01, 0.03, 0.05$), 20 mL of deionized water was placed in a beaker and heated to 60°C . Then, 1 mL of concentrated nitric acid was added. Following this, the required amounts of $\text{Fe}(\text{NO}_3)_3 \cdot 9\text{H}_2\text{O}$ (1.99 g, 1.95 g, 1.91 g), $\text{Bi}(\text{NO}_3)_3 \cdot 5\text{H}_2\text{O}$ (2.52 g), and $\text{Ni}(\text{NO}_3)_2 \cdot 6\text{H}_2\text{O}$ ($x = 0.01, 0.03, 0.05$) were mixed together. After these salts completely dissolved, 1.5 g of tartaric acid ($\text{C}_4\text{H}_6\text{O}_6$) was added, resulting in the formation of a mustard-colored colloidal solution. The pH of the solution was then adjusted to 3 by adding ammonia, yielding a lemon-colored solution.

The materials were then ground and placed in a crucible, which was heated in a furnace at 400°C for 3 hours. After cooling, the materials were washed with acid and then placed in the furnace again at 650°C for 4 hours. Finally, the sample was analyzed using XRD to determine its crystalline structure.

2-5- Photocatalytic procedure

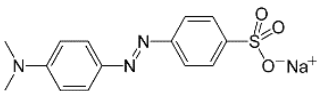
The photocatalytic activity of BFO nanoparticles and nickel-doped BFO was investigated for the degradation of methylene orange in an aqueous solution under different light exposures and at room temperature. Initially, calibration steps were performed to determine the concentration of methylene orange (3 mg/L), which was used for the experiments. Then, 300 mL of the methylene orange solution at the determined concentration was transferred into a 600 mL beaker, and after adding the nano catalyst and hydrogen peroxide to the beaker, the pH was adjusted to different values using HCl and NaOH. Afterward, the beaker was placed inside a photoreactor, and the solutions were stirred for 30 minutes at 750 rpm under dark conditions. Every 20 minutes, 3 mL samples were taken using a pipette and transferred into a clean, dry centrifuge tube. The samples were then centrifuged at 4000 rpm for 10 minutes to separate the suspended photocatalyst particles. Finally, the solution was transferred into the UV-Vis spectrophotometer cell, and the absorption spectrum of the solution was recorded in the range of 200 to 800 nm. The mercury vapor lamp was then turned on, and the solution was exposed to the light. The experiments were performed using a homemade photoreactor equipped with a mercury vapor lamp and a magnetic stirrer. The distance between the lamp and the stirrer was 18 cm. During each step, the absorbance of the methylene orange solution was measured at a wavelength of 461 nm (the maximum absorption wavelength of methylene orange in water). The photocatalytic degradation efficiency was calculated based on the percentage of methylene orange degradation using the following equation [14]:

Methylene Orange Degradation (%)= $\frac{c_0 - c_t}{c_0} \times 100$

Equation 1 - Percentage Degradation of Methyl Orange

In this equation, C₀ and C_t represent the initial concentration of the dye and the concentration at time t (0–120 minutes) after lamp irradiation, respectively.

Table1. Physical and Chemical Properties of Methyl Orange Dye (MO)

Parameters Methyl orange	
Molecular formulae	C ₁₄ H ₁₄ N ₃ NaO ₃ S
molar mass	327.33g/mol
Appearance	red powder
Structure	

3- Results and discussion

3-1-Investigation of Factors Affecting the Photocatalytic Activity of Nickel-Substituted Bismuth Ferrite in Methyl Orange Degradation

The degradation of methyl orange dye was investigated and measured under the influence of pH, nanoparticle dosage, and irradiation time. Experimental results demonstrated that nickel-substituted BFO nanoparticles exhibit high efficiency in the degradation of methyl orange dye, attributed to their unique chemical properties and narrow energy band gap [15]. Optimization of the parameters revealed that the degradation efficiency of methyl orange by BiFe_{0.97}Ni_{0.03}O₃ reached 76.33% within 120 minutes.

3-2- The Effect of pH

The pH of the dye solution has a significant influence on the interaction between the adsorbent surface and dye molecules, affecting their attachment to the solid surface. This phenomenon is primarily attributed to the effect of pH on the surface characteristics of the adsorbent, as well as the dissociation and ionization behavior of the adsorbate molecules. Since adsorption of a dye or pollutant onto the catalyst is the initial and critical step in the degradation process, it is closely related to the zero-point charge pH (pH_{pzc}) of the catalyst and the ionic nature of the pollutant [16].

In this phase of the study, a specific concentration of methyl orange solution was prepared and transferred into a beaker. A known amount of catalyst was added, followed by the addition of 0.5 mL of H₂O₂. The effect of pH was investigated at levels 2, 3, and 4. Based on the experimental results, pH = 2 was identified as the optimum value for the degradation process (Fig. 1). This can be attributed to the anionic nature of methyl orange and the increased positive charge on the catalyst surface under acidic conditions, which facilitates stronger electrostatic attraction between the catalyst and dye molecules, thereby enhancing adsorption and degradation efficiency.

Conversely, at pH values higher than the optimum, degradation efficiency decreased. This reduction is due to the increase in negative surface charge of the catalyst, leading to electrostatic repulsion between the catalyst and the anionic dye molecules, which in turn reduces adsorption and the subsequent degradation performance.

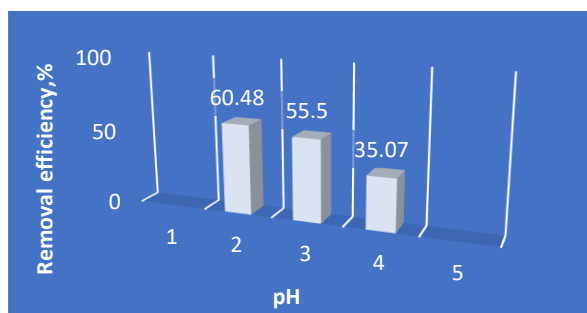


Fig.1. The percentage degradation rate of methyl orange (MO) at different pH levels (2, 3 & 4) was investigated. The experimental conditions included an MO concentration of $3 \text{ mg} \cdot \text{L}^{-1}$, 0.50 mL of H_2O_2 , 0.10 g of pure BFO nanoparticles, and exposure to UV light irradiation.

3-3- The effect of irradiation

The procedure was as follows: initially, a specified amount of methyl orange was transferred into a beaker after adjusting the volume. Then, BFO nanoparticles were added, followed by the addition of 0.5 mL of hydrogen peroxide. The pH was then adjusted, and the solution was transferred to the photochemical reactor. Degradation was measured at various time intervals (Fig.2). This process showed that with an increase in time, the percentage of dye degradation increased. However, over time, the adsorption rate on the solid surface and the molecules in the solution phase decreased. This phenomenon indicates that the catalyst reached saturation, and its capacity to accept new molecules was exhausted. Moreover, the increase in adsorption can be attributed to the frequency of collisions between the pollutant and the catalyst. As the residence time increases, the likelihood of collisions grows, leading to enhanced pollutant adsorption by the catalyst.

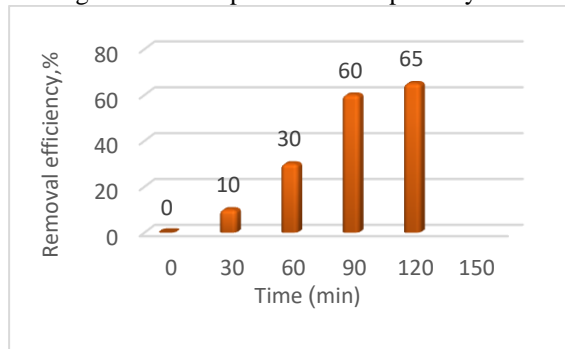


Fig.2. Degradation efficiency of methyl orange dye over 30–120 minutes using 0.1 g nanoparticles, 0.5 mL H_2O_2 , 300 mL of 3 mg/L dye solution at pH 2 under mercury lamp irradiation

3- 4- The effect of catalyst amount

Figure 3 shows that in the absence of BFO nanoparticles, the degradation is minimal, indicating the crucial role of the nanoparticles. To optimize the amount of nanoparticle, various quantities (0 , 0.05 , 0.10 , 0.15 , and 0.20 g) were tested. The results revealed that 0.1 g of the catalyst is the optimal amount. As the amount of catalyst increased to 0.1 g , the number of active sites on the catalyst surface also increased, leading to a higher degradation rate of the dye. However, when the nanoparticle amount increased to 0.15 g and 0.2 g , turbidity formed in the solution due to the higher concentration of nanoparticles. The resulting turbidity caused light scattering in the solution, which prevented photons from penetrating deeply into the solution. As a result, the rate of photocatalytic degradation reactions decreased.

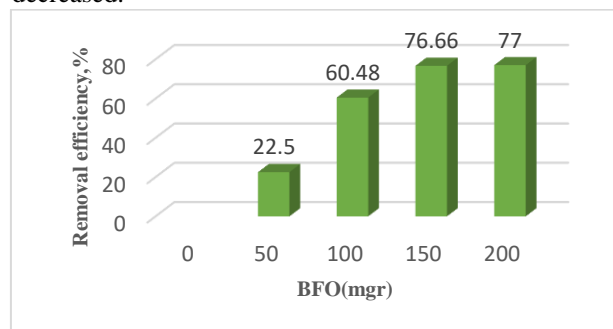


Fig.3. The rate of percentage of degradation of MO at different catalyst dosages (0 , 0.05 , 0.10 , 0.15 & 0.20 g). Experimental conditions: concentration of 3 mg L^{-1} of MO, 0.50 mL H_2O_2 , under UV light irradiation and pH 2

3-5-The performance of nickel-doped bismuth ferrite (BFO) in the removal of methyl orange dye was investigated by using different concentrations of nickel

In this study, the effect of different nickel doping concentrations (1%, 3%, and 5%) on bismuth ferrite (BFO) for the removal of methyl orange dye was investigated. For this purpose, 0.01, 0.03, and 0.05 g of nickel were doped into the BFO, and each sample was mixed with 0.1 g of nanoparticles and 0.5 mL of hydrogen peroxide. The solution was then exposed to the photoreactor under UV light at pH = 2 for 2 hours. Afterward, the methyl orange dye degradation was monitored at a wavelength of 461 nm using a spectrophotometer.

The results showed that after a 120-minute reaction time, the degradation percentage of methyl orange reached 76.33% for the 0.03% nickel-doped BFO, which was the highest degradation rate among the other samples. This increase in adsorption and dye removal over the defined time period can be attributed to the enhancement of the photocatalytic activity of bismuth ferrite with nickel doping. The improvement in photocatalytic performance is related to the change in nanoparticle size and the alteration of the structure of bismuth ferrite due to nickel substitution.

4- The structure of the synthesized photocatalysts

4-1- FE-SEM analysis of BFO

The results obtained from the (FE-SEM) analysis, shown in Figure 4, are used to examine the morphology and determine the size of the synthesized particles. For Bismuth Ferrite (BFO), the images indicate that in the absence of nickel and with varying nickel substitution percentages, the nanoparticles are in the nanoscale range with smooth surfaces and uniform particle distribution. The images revealed that as the nickel substitution percentage in the BFO structure increased, the synthesized nanoparticles took on irregular shapes with different particle sizes. Additionally, the particle size decreased with increasing nickel content. Furthermore, the pore size of the BFO nanoparticles decreased with the increase in nickel substitution, which led to an enhanced selectivity for the penetration of molecules in the sample solution, such as pollutants, into the BFO network. This structural modification likely contributed to improved photocatalytic performance, as smaller pores can offer a greater surface area for interactions between the catalyst and the pollutants.

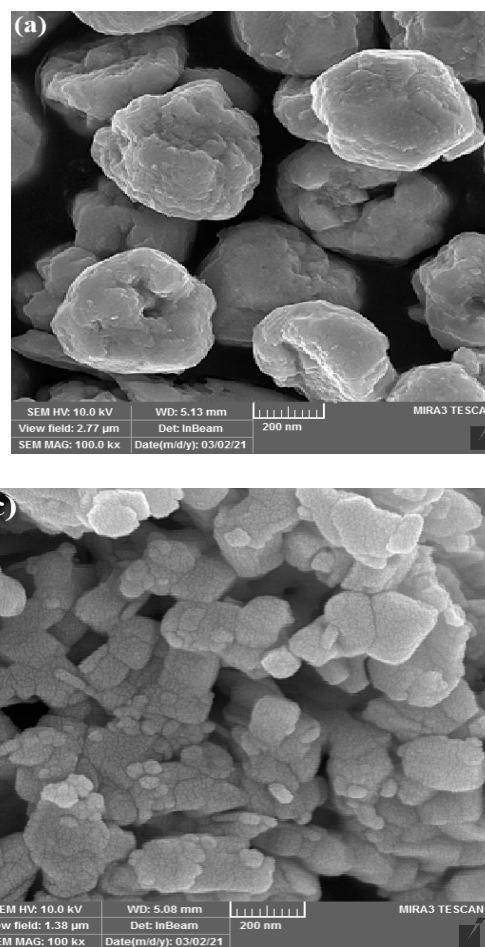


Fig. 4[17] FE-SEM images of nanoparticles: (a) BFO(c) $\text{BiFe}_{0.97}\text{Ni}_{0.03}\text{O}_3$

4-2- XRD analysis

The main objective of this study is to investigate the effect of BFO (Bismuth Ferrite) on the removal of methyl orange dye. The XRD patterns of BFO, shown in Figure 5, reveal that the BFO structure exhibits a perovskite structure with the space group R_{3c} . The XRD spectra of the samples were compared with those of other recorded samples using XPert software, as shown in the diagram below. As observed in Figure 5, the results indicate that nickel doping in bismuth ferrite leads to a slight improvement in the photocatalytic activity. The XRD analysis suggests that the doping of nickel into the BFO structure causes minor modifications in the crystallinity and phase composition, which could enhance the photocatalytic degradation of methyl orange dye. The increase in photocatalytic activity is likely due to the changes in the structural properties induced by the nickel substitution, which affect the catalyst's surface area, charge carrier dynamics, and light absorption characteristics.

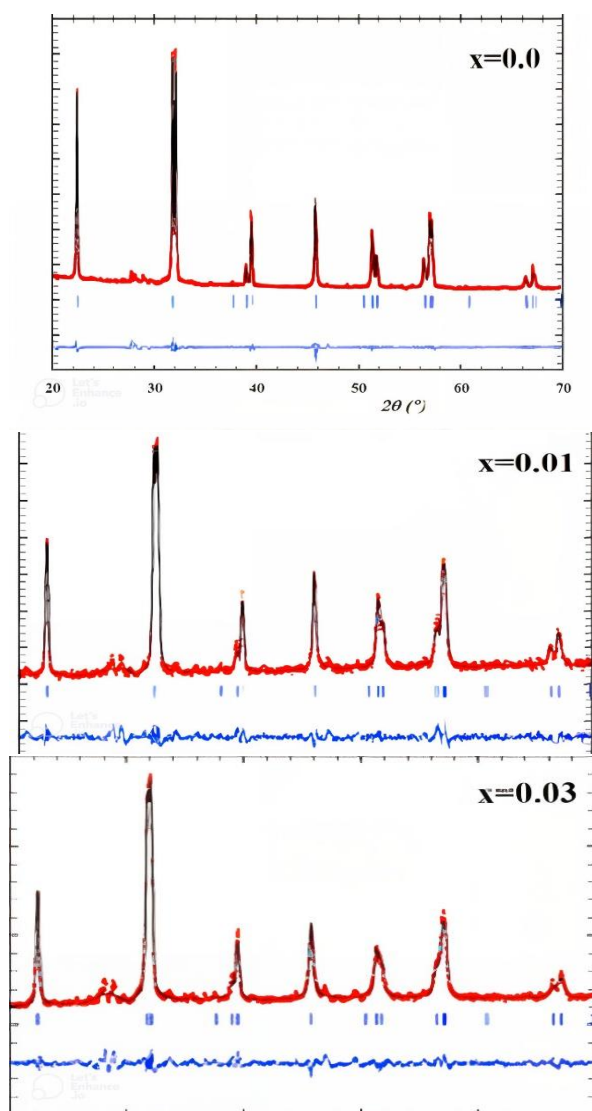


Fig. 5. XRD patterns with the perovskite schematic and R_{3C} space group for the nanoparticles [17] BiFeO_3 , $\text{BiFe}_{0.99}\text{Ni}_{0.01}\text{O}_3$, $\text{BiFe}_{0.97}\text{Ni}_{0.03}\text{O}_3$

4-3- FT-IR spectrum

FT-IR analysis was performed to identify the functional groups present in the synthesized photocatalysts, as shown in Fig.6. The FT-IR spectrum of the pure BFO sample exhibits distinct absorption bands around 564.32 cm^{-1} , 589.45 cm^{-1} , and 419.31 cm^{-1} , which are attributed to the stretching and bending vibrations of Fe–O bonds. These bands confirm the presence of FeO_6 octahedral units in the perovskite structure. Additionally, a broad band observed near 3449.95 cm^{-1} corresponds to the stretching vibration of hydroxyl groups ($\nu(\text{O-H})$), indicating moisture adsorption or the presence of surface–OH groups. In the spectrum of the Ni-doped sample ($\text{BiFe}_{0.97}\text{Ni}_{0.03}\text{O}_3$), similar vibrational bands related to Fe–O bonds appear at approximately 565.12 cm^{-1} and 614.19

cm^{-1} , accompanied by slight shifts. This shift may indicate lattice distortion caused by the incorporation of Ni ions. Furthermore, the broad band at 3436.43 cm^{-1} is associated with the stretching vibration of surface –OH groups ($\nu(\text{O-H})$), while the absorption band at 1631.51 cm^{-1} corresponds to the bending vibration of molecular water ($\delta(\text{O-H})$). These features confirm the successful formation of the perovskite phase and the presence of surface hydroxyl groups, which play a key role in photocatalytic activity

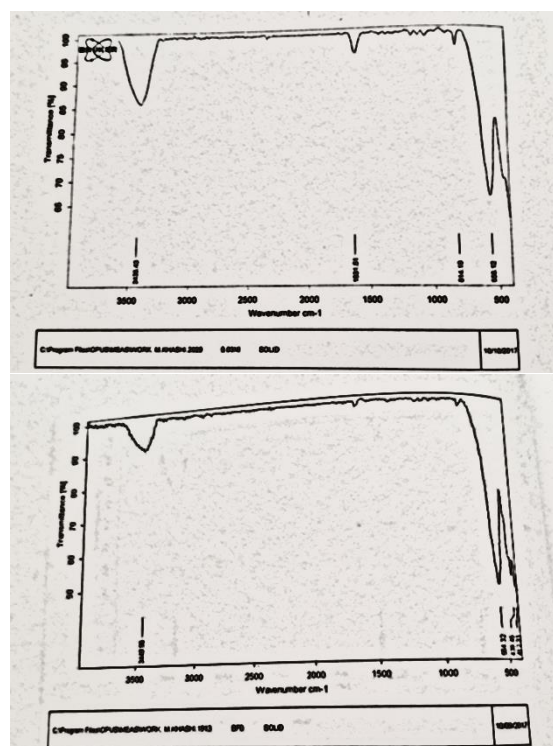


Fig.6. FT-IR spectrum of the un-doped and $\text{BiFe}_{0.97}\text{Ni}_{0.03}\text{O}_3$

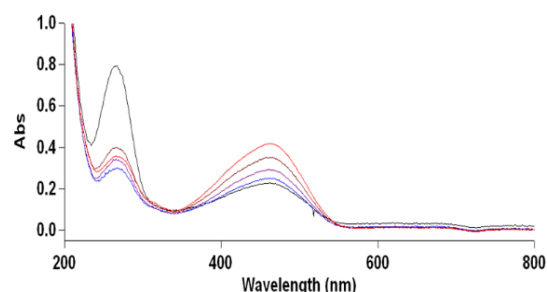


Fig.7. UV-Vis spectrum ($\lambda_{\text{max}} = 461\text{ nm}$) after 120 min under optimal conditions: BFO = 0.1 g, pH = 2, dye = 3 ppm.

5-kinetic study

For this purpose, the pseudo-first-order rate constant for the photodegradation of Methyl Orange was determined

based on the following linear equation (Lente, 2018). In this equation, A and k represent the absorbance of Methyl Orange at a given irradiation time and the pseudo-first-order rate constant respectively. Additionally, X and E denote the amplitude and the endpoint of the photodegradation process, both having the same unit as the measured quantity A

$$A = Xe^{-kt} + E$$

Equation 2

Various strategies have been employed to enhance the efficiency of the photocatalytic process, mainly by optimizing the kinetics of pollutant degradation. These strategies include the proper selection of photocatalysts, doping with specific elements or compounds, coupling with other semiconductors, modifying the crystal structure and morphology, and improving surface properties. In this study, various parameters were investigated and analyzed to achieve maximum efficiency in the photocatalytic degradation of methyl orange. In this context, doping with nanoparticles, metal ions, and nanocomposites significantly enhances the performance of semiconductors. To achieve this goal, a comparative investigation was performed on the photocatalytic degradation of methyl orange employing BFO nanoparticles doped with different concentrations of Ni ions (0.01, 0.03, and 0.05). The photocatalytic performance of these nanoparticles in the degradation of methyl orange was compared in Figure 8 for different Ni doping concentrations of 1%, 3%, and 5%. The degradation efficiencies of methyl orange in $\text{BiFe}_{1-x}\text{Ni}_x\text{O}_3$ samples with $x = 0.01, 0.03, \text{ and } 0.05$ were 74.4%, 76.33%, and 76%, respectively, after 120 minutes under optimized conditions. Therefore, the highest degradation of methyl orange within the shortest time was achieved using the Ni-doped BFO photocatalyst with 3% nickel content. This finding correlates well with the optical bandgap values of the samples. Moreover, high concentrations of Ni and other dopants may lead to the

formation of recombination centers within the BFO lattice, resulting in a decrease in the photocatalytic activity of the nanoparticles. The results demonstrated that the presence of Ni dopant ions in the BFO lattice structure significantly enhances the reaction rate of methyl orange degradation. It was anticipated that Ni-doped BFO would exhibit superior photocatalytic performance compared to undoped BFO in the degradation of methyl orange.

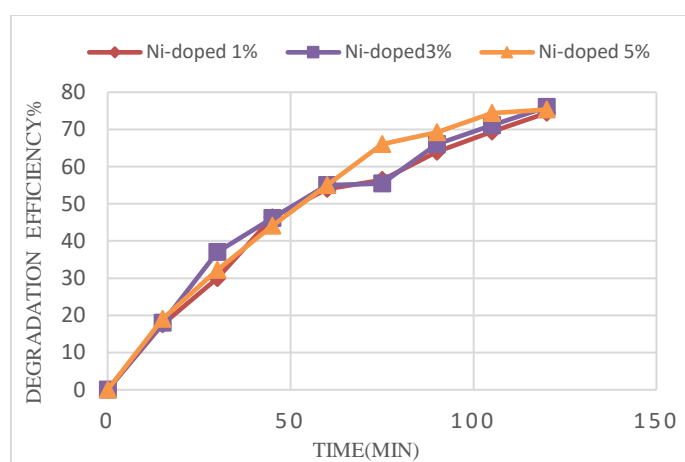
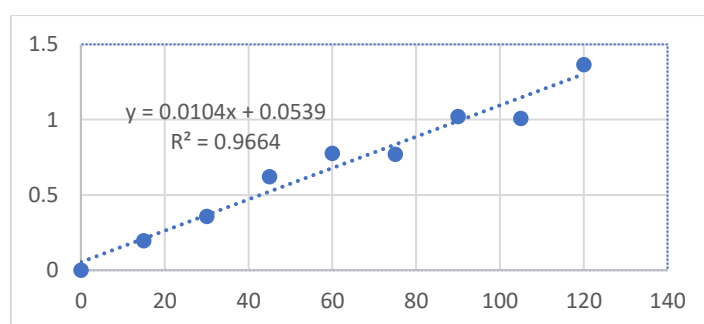
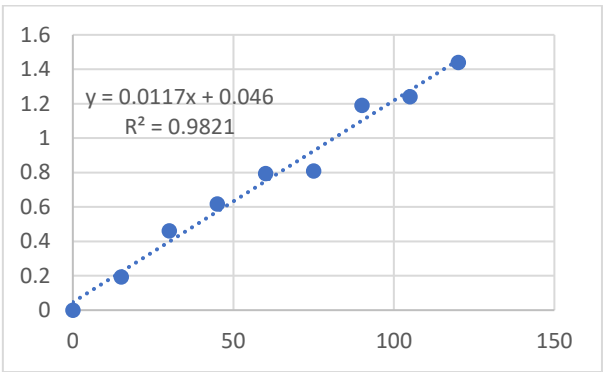


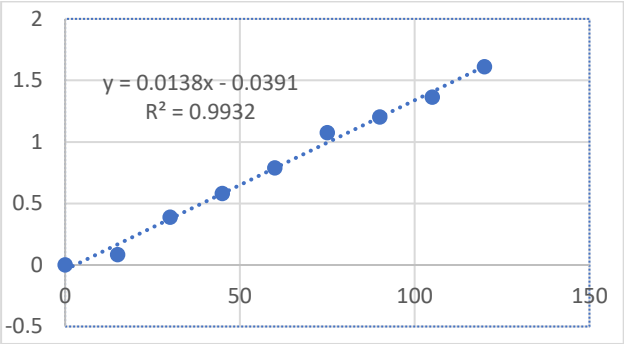
Fig.8. Photocatalytic degradation of methyl orange using Ni-doped BiFeO_3 nanoparticles (0.01, 0.03 & 0.05 doping) under UV light at pH 2, with 3 mg/L dye and 0.1 g catalyst



a) pseudo-first-order reaction kinetics of photocatalytic degradation of methyl orange dye 1%



b) pseudo-first-order reaction kinetics of photocatalytic degradation of methyl orange dye 3%



c) pseudo-first-order reaction kinetics of photocatalytic degradation of methyl orange dye 5%

Table2. The data for the pseudo-first-order kinetics equation,

Ni- BFO	R ²	k (min ⁻¹)
BiFe _{0.99} Ni _{0.01} O ₃	0.9664	0.0104
BiFe _{0.97} Ni _{0.03} O ₃	0.9821	0.0117
BiFe _{0.95} Ni _{0.05} O ₃	0.9932	0.9932

Table3. Comparison other catalyst activity in

Catalyst	Method	Source	pH	Time (min)	%RE	Ref
Ag-modified Cr-doped BaTiO ₃ aerogel	co-gelation	Solar simulator, 420 W xenon lamp	3	60	92	[18]
TiO ₂ -NPs	Green synthesis	UV	7	210	92	[19]
SnO ₂ /TiO ₂	Hydrothermal	Xenon	2	120	91	[20]
Titanium nanotube array (non-ferrous Fenton system)	Non-ferrous Fenton photocatalysis	Simulated solar light, 100 mW/cm ² , AM 1.5G spectrum	3	60	99.7	[21]
Present Work	Sol-Gel	UV-A	2	120	76.33	-

5. Conclusion

In this study, nickel-doped bismuth ferrite (BFO) nanoparticles from the perovskite oxide family were synthesized using the sol-gel method. The structural and morphological properties of BFO were characterized by X-ray diffraction (XRD) spectroscopy, which indicated the R₃C structure [22], and by Field Emission Scanning Electron Microscopy (FE-SEM). The FE-SEM images reveal that the BFO nanoparticles exhibit a uniform distribution of sizes and a consistent structure [23]. The BFO nanoparticles were then used as a photocatalyst for the degradation of methyl orange dye [24], and the process was studied using UV-Vis spectroscopy. In this project, key parameters influencing the degradation efficiency of methyl orange dye, including pH, dye concentration, catalyst amount, and irradiation time, were examined and optimized. The optimal conditions were found to be: mercury lamp irradiation with an intensity of 250 watts, dye concentration of 3 mg/L, 0.1 g of photocatalyst, and a solution pH of 2. During the degradation process of methyl orange dye by the synthesized catalysts, BiFe_{0.97}Ni_{0.03}O₃ (nickel-doped bismuth ferrite) achieved a degradation rate of 76.33% after 120 minutes, demonstrating the effectiveness of this catalyst for dye removal.

References

- [1] E. Routoula, S. V. Patwardhan, Degradation of anthraquinone dyes from effluents: A review focusing on enzymatic dye degradation with industrial potential, *Environmental Science & Technology*, 54 (2020) 647-664.
- [2] M. Anjum, M. Abbas, M. B. K. Niazi, R. A. Khan, Remediation of wastewater using various nanomaterials, *Arabian Journal of Chemistry*, 12 (2019) 4897-4919.
- [3] Z. Aksu, A. İ. Tatlı, Ö. Tunç, A comparative adsorption/biosorption study of Acid Blue 161: Effect of temperature on equilibrium and kinetic parameters, *Chemical Engineering Journal*, 142 (2008) 23-39.
- [4] F. Shahrab, A. Tadjarodi, Novel magnetic nanocomposites BiFeO₃/Cu (BDC) for efficient dye removal, *Heliyon*, 9 (2023) 45974-45982.
- [5] P. Bhattacharya, A. Barik, L. Acharya, S. Dasgupta, Disinfection of drinking water via algae-mediated green synthesized copper oxide nanoparticles and its toxicity evaluation, *Journal of Environmental Chemical Engineering*, 7 (2019) 102867.
- [6] N. Abidi, H. Mokhtari, M. Ghorbani, S. Abbasi, Treatment of dye-containing effluent by natural clay, *Journal of Cleaner Production*, 86 (2015) 432-440.
- [7] S. Abbasi, M. Hasanpour, The effect of pH on the photocatalytic degradation of methyl orange using decorated ZnO nanoparticles with SnO₂ nanoparticles, *Journal of Materials Science: Materials in Electronics*, 28 (2017) 1307-1314.
- [8] B. Ruetter, B. Kundys, V. Dhanasekharan, J. F. Scott, Magnetic-field-induced phase transition in BiFeO₃ observed by high-field electron spin resonance: Cycloidal to homogeneous spin order, *Physical Review B*, 69 (2004) 064114.
- [9] W. Eerenstein, N. Mathur, J. F. Scott, Multiferroic and magnetoelectric materials, *Nature*, 442 (2006) 759-765.
- [10] X. Wang, Y. g. Zhang, Z. Wu, Magnetic and optical properties of multiferroic bismuth ferrite nanoparticles by tartaric acid-assisted sol-gel strategy, *Materials Letters*, 64 (2010) 486-488.
- [11] S. Mousavi et al., Nanofiber-immobilized CeO₂/dendrimer nanoparticles: An efficient photocatalyst in the visible and the UV, *Applied Surface Science*, 479 (2019) 608-618.
- [12,13] M. Iddique, N. M. Khan, M. Saeed, Photocatalytic activity of bismuth ferrite nanoparticles synthesized via sol-gel route, *Zeitschrift für Physikalische Chemie*, 233 (2019) 595-607.
- [14] S. M. Tichapondwa, J. Newman, O. Kubheka, Effect of TiO₂ phase on the photocatalytic degradation of methylene blue dye, *Physics and Chemistry of the Earth, Parts A/B/C*, 118 (2020) 102900.

- [15] C. Ponraj, G. Vinitha, J. Daniel, A review on the visible light active BiFeO₃ nanostructures as suitable photocatalyst in the degradation of different textile dyes, *Environmental Nanotechnology, Monitoring & Management*, 7 (2017) 110-120.
- [16] L. Esmaili, Effect of temperature and concentration of bismuth nitrate mole on structural, magnetic and photocatalytic properties of bismuth ferrite, *Iranian Journal of Crystallography and Mineralogy*, 26 (2019) 1013-1026.
- [17] M. V. Neshin, R. S. Khoshnood, D. S. Khoshnoud, Enhanced photocatalytic activity of Ni-doped BiFeO₃ nanoparticles for degradation of bromophenol blue in aqueous solutions, *Reaction Kinetics Mechanisms and Catalysis*, 134 (2021) 951-970.
- [18] J. Wu, G. Shao, X. Wu, S. Cui, X. Shen, Ag-Incorporated Cr-Doped BaTiO₃ Aerogel toward Enhanced Photocatalytic Degradation of Methyl Orange, *Nanomaterials*, 14 (2024) 848.
- [19] R. Putri, I. Safitri, M. Sofyan, D. Deliza, Sol-gel Mediated by Extract of Santang Orange Peel in Synthesis of TiO₂ Nanoparticle for Photocatalytic Degradation of Methyl Orange, *Moroccan Journal of Chemistry*, 13 (2025) 463-479.
- [20] H. Huang, S. Zhao, Y. Yang, Y. Wang, R. Lu, Y. Lu, J. Chen, Axially wrinkled tubular SnO₂/TiO₂ heterostructures for effective degradation of organic pollutants, *Materials Science in Semiconductor Processing*, 152 (2022) 107065.
- [21] S. Zavahir, T. Elmakki, N. Ismail, M. Gulied, H. Park, D. S. Han, Degradation of organic methyl orange (MO) dye using a photocatalyzed non-ferrous Fenton reaction, *Nanomaterials*, 13 (2023) 639.
- [22] A. Saghafi, R. S. Khoshnood, D. S. Khoshnoud, Z. Es'Haghi, Magnetic properties and photocatalytic activity of Bi_{1-x}Sm_xFe_{1-y}Ni_yO₃ nanoparticles for methyl red degradation, *Reaction Kinetics, Mechanisms and Catalysis*, 135 (2022) 3375-3391.
- [23] M. V. Neshin, R. S. Khoshnood, S. Akbari, Investigation on the photocatalytic activity of bromophenol blue using Cr-doped BiFeO₃ nanoparticles in aqueous solutions by UV-Vis spectrophotometry, *Russian Journal of Physical Chemistry A*, 97 (2023) 2434-2442.
- [24] Elaheh K. F., Seyyedali H. Z. T., Mojtaba N., The effect of pH on the adsorption properties of ZnO-CdO nanoparticles for the removal of methyl blue and methyl orange, *Journal of Novel Processes in Materials Engineering*, 11 (2017) Spring.